Biochimica et Biophysica Acta, 778 (1984) 1–16
Elsevier

BBA 72284

KINETICS AND pH-DEPENDENCE OF GLYCINE-PROTON SYMPORT IN *SACCHAROMYCES CEREVISIAE*

A BALLARIN-DENTI *, J A DEN HOLLANDER **, D SANDERS §, C W SLAYMAN and C L SLAYMAN §§

Departments of Human Genetics, Molecular Biophysics and Biochemistry, and Physiology, Yale University, New Haven, CT 06510 (U S A)

(Received May 3rd, 1984)

Key words Amino acid transport, Glycine/H^+ symport, Intracellular pH, ^{31}P-NMR, Kinetics, (*S cerevisiae*)

Interactions between intracellular pH (pH_i) and H^+-coupled transmembrane transport of glycine have been studied by means of ^{31}P-NMR, using both aerobic and 'energy starved' cells of the yeast *Saccharomyces cerevisiae*. The general features of glycine transport in the yeast strain used (NCYC 239) are similar to those already reported for *Saccharomyces carlsbergensis* and *S. cerevisiae*, there being two kinetically distinct glycine uptake systems, with pH-independent $K_{1/2}$ values near 14 and 0.4 mM, respectively, but pH-dependent maximal velocities. Glycine transport itself has no measurable effect on pH_i in aerobic cells, and only a marginal effect in energy-starved cells, but changes of pH_i, imposed by extracellular addition of butyric acid, strongly influence glycine transport. Indeed, the dependence of glycine influx (in energy-starved cells) upon cytoplasmic H^+ concentration appears to be third order, showing Hill slopes of 2.7–3.0. A crucial kinetic role for cytoplasmic pH in glycine transport is further indicated by a proportionality between the decline of flux and the decline of pH_i produced by various metabolic inhibitors and uncouplers. Extracellular pH (pH_o), by contrast, has only a weak effect on glycine influx, showing a Hill slope of 0.5. The major observations can be accommodated by a simple cyclic carrier scheme, in which 2 or more protons are transported along with glycine, but only one extracellular proton binding site dissociates in the testing range, with a pK near 5.5. The model requires a finite membrane potential, which must be somewhat sensitive to both pH_i and pH_o, and accommodates the discrepancy between measured net proton flux (one per glycine) and the kinetically required proton flux (two or more per glycine) by shunting through other proton-conducting pathways in the yeast membrane.

Introduction

There is now almost overwhelming evidence, of both kinetic and thermodynamic nature, for cotransport of protons along with various solutes into bacterial, fungal, algal, and higher plant cells, as was originally postulated by Mitchell [1] Examples that have been studied in detail include lactose transport in *Escherichia coli* [2,3], glycine transport in *Saccharomyces* [4] and *Lemna gibba* [5], glucose transport in *Neurospora* [6] and *Chlorella* [7], sucrose transport in *Ricinus* cotyledons [8,9] and *Samanea* pulvini [10], and a variety of amino acids in *Avena* coleoptiles [11]. In all of these cases, solute entry into the cells is accompanied by uptake of protons and by depolarization of the plasma membrane; and maximal steady-state levels of ac-

* Current address Dipartimento di Biologia, Università degli Studi di Milano, Milano, Italia
** Current address Max-Planck-Institut fur Systemphysiologie, Rheinlandamm 201, D-4600 Dortmund 1, F.R G.
§ Current address. Department of Biology, University of York, Heslington, York, U.K
§§ To whom correspondence should be addressed

cumulated solute appear quantitatively related to the energy available from the electrochemical gradient of protons [6,11–13].

Nevertheless, numerous questions concerning both physiological and molecular mechanisms of proton cotransport remain unanswered In particular, the magnitude of solute-dependent proton flux has been unequivocally defined in only one or two systems; and the physiological consequences of that flux are matters of speculation only This is so in part for methodological reasons solute-coupled proton flux is usually deduced from alkalinization of extracellular medium, since sufficiently rapid and sensitive methods for measuring the expected changes of intracellular pH have not generally been available. But metabolic factors also introduce considerable uncertainty into the measurement of proton fluxes. In yeast, for example, Eddy and Nowacki [14] and Seaston et al. [15] observed maximal uptake of protons associated with glycine transport (stoichiometry of 2 H^+ . 1 glycine) only when energy metabolism had been completely blocked by the simultaneous presence of 2-deoxyglucose and antimycin A With partial energy restriction (absence of inhibitors, but also absence of glucose), glycine stimulated a smaller proton flux (stoichiometry of about 1 : 1) And under energy-replete conditions (glucose and oxygen abundant, no inhibitors present), addition of glycine caused no significant deflection of the extracellular pH trace These observations were interpreted to mean that, whenever sufficient metabolic energy is available, protons entering the cells via the glycine cotransport system are pumped out almost immediately, presumably by an electrogenic proton pump, which has been identified in yeast and other fungal membranes [16,17]. But neither a direct demonstration of accelerated proton pumping nor any evidence for appropriate cytoplasmic acidification, in the presence or absence of metabolic energy, has been given

A second, related, problem concerns possible effects of changes in intracellular pH on the behavior of the cotransport system itself Komor et al. [18] have shown that in *Chlorella* a drop in intracellular pH, brought about by addition of uncouplers, caused severe inhibition of H^+-dependent hexose cotransport And Sanders and Hansen [19], using internally perfused internodal cells of the giant alga *Chara corallina*, demonstrated that lowered intracellular pH likewise suppresses H^+-dependent chloride uptake. In both cases the effect could be described by a simple carrier model of cotransport in which binding and release of the solute and protons are strictly ordered: hexose (or chloride) binding before protons at the outside surface of the membrane and releasing first at the inside surface [19,20] The possibility that a similar, ordered mechanism might operate in yeast is intriguing

Obviously, any systematic approach to these questions demands measurement and control of intracellular pH (pH_i), as well as extracellular pH (pH_o). Slow or static measurements of pH_i have been accomplished on yeast, algae, and bacteria by using weak acids as distribution indicators [15,18,21,22], and intracellular microelectrodes, which generally give much greater sensitivity and time resolution, have become available for use with the larger cells of *Neurospora* and the giant algae [23,24] But a technique which appears to have more general applicability is nuclear magnetic resonance of phosphorus-31 (^{31}P-NMR, [25,26]). Thus far it has been used on yeast to map phosphorylated intermediates and explore the behavior of pH_i with respect to glycolysis, oxidative metabolism [27,28], cell division [29], sodium and potassium transport [30] and phosphate transport and vacuolar partitioning [31,32] It has also been used to extract reaction rate constants for ATP synthesis [33]. The speed (temporal resolution of 15 s or less), sensitivity (pH resolution of about 0 03 unit), and non-invasive nature of ^{31}P-NMR make it very attractive for study of transport, and the experiments described below were initiated to take advantage of this technique in order to resolve some of the main questions concerning pH_i and proton-dependent solute transport

Glycine uptake by the general amino acid permease of yeast was chosen for study, because of the extensive background information (about substrate specificity, stoichiometry, and energy-dependence) already available, largely from the work of Eddy and his collaborators (see review by Eddy [4]). A surprising initial result was obtained· that the change of intracellular pH which should accompany the proton-coupled transport is barely measurable. This finding (paralleled by results on

glucose-proton cotransport in *Neurospora*, obtained with pH-microelectrodes (Sanders, D., unpublished observations)) prompted detailed measurements of cytoplasmic buffer capacity, ionic exchange, metabolic dependence, and pH_i-dependence of glycine flux in *S cerevisiae*, in order to determine whether the glycine uptake system in that species is in fact functionally equivalent to the more extensively studied system in *S carlsbergensis* [15,34] The results obtained permit proton-glycine cotransport in *S cerevisiae* to be formally described by a simple Class-I charge-dependent carrier mechanism [20,35] having a proton : glycine stoichiometry of 3 1 (2 1 or greater), with ordered binding and release of ligands

Experimental Procedures

Cells Strain NCYC 239 of *Saccharomyces cerevisiae* was used in this work and was maintained according to the procedures of Eddy et al. [12] Cells were grown on a reciprocating shaker at 25 °C, following inoculation into liquid medium containing mineral salts and 2% glucose, with ammonium sulfate as the nitrogen source. When suspensions had reached a density of about 5 g wet weight of cells per liter (late log-phase), the cells were harvested by centrifugation ($1000 \times g$ for 3 min), washed twice and resuspended as a dense slurry (1 part cells : 1 part water) in ice-cold distilled water, then stored at 4 °C for up to 18 h Before most experiments, suspensions were brought to 30 °C for 40–60 min, by addition of standard buffer medium (see below) containing 100 mM glucose. Thereafter, the cells were recollected, washed, suspended in distilled water, and stored (for up to 1 h) at 4 °C For experiments, rewashed cells were again mixed with standard buffer medium, at controlled densities between 2 and 25 mg dry wt /ml medium.

Buffer solutions. The standard buffer medium for flux experiments on energy-replete cells was 20 mM Tris citrate at pH 4 5; for energy-restricted (starved) cells, antimycin A (0.5 μg/mg dry wt. of cells) and 2-deoxyglucose (5 mM) were added to standard buffer medium The suspensions were bubbled with 95% O_2/5% CO_2 for experiments with aerobic cells, and with 95% N_2/5% CO_2 for experiments with anaerobic or starved cells Solutions buffered at other pH values were prepared by titrating 20 mM Tris hydroxide with the required amount of citric acid In preliminary experiments, other buffer solutions, such as 20 mM dimethylglutaric acid supplemented with 1 mM $CaCl_2$ [36], were tested and found equivalent to standard buffer medium for glycine-, H^+-, and K^+-flux measurements.

Isotope measurements Buffered cell suspensions were pre-equilibrated on the reciprocating shaker (30 ° C, 90 cycles/min; ± inhibitors, as indicated in the figure legends) for 5–10 minutes, after which glycine uptake was initiated by addition of ^{14}C-labelled glycine (New England Nuclear Corp.) at final specific activities of 0.003–3 0 μCi/mol, depending on the total glycine concentration. At appropriate intervals, 1-ml samples were withdrawn and rapidly mixed with 7 ml of ice-cold 20 mM Tris-citrate at pH 7.1, as described by Eddy et al [12]. Cells were harvested by centrifugation, washed twice with iced buffer, and extracted in hot distilled water (2 ml, 95 ° C, 15 min). 0 3-ml aliquots were subsequently diluted into 5 ml of Aquasol (New England Nuclear Corp) and assayed for radioactivity with a Beckman LS-3150T liquid scintillation counter Control experiments revealed no significant leakage of radioactivity from the cells during washing, so that more than 95% of the total radioactivity was carried into the extraction fluid.

Potassium and proton fluxes. For ion fluxes associated with glycine transport, cells were suspended in buffer at a density of 15–25 mg dry wt /ml and poured into a water-jacketed vessel (30 ° C, 30 ml) containing a glass pH electrode, a PVC-K^+ electrode (see below), and an NaCl bridge to the reference electrode. (1 M NaCl was used in the bridge, in order to avoid potassium leakage from a standard 3 M KCl bridge.) The two ion-specific electrodes and the reference electrode were connected to two chopper-stabilized high impedance amplifiers (Radiometer pH Meter 22), and thence via a simple divider/compensator network to a chart recorder (Texas Instruments Servoriter II).

Changes of pH and K^+ concentration in the medium were recorded as functions of time, and were calibrated at the end of each experimental run by addition of 1–5 μequivalents of HCl,

NaOH, or KCl to the cell suspension. This simple calibration procedure was adequate, because the buffering capacity of yeast suspensions proved to be sensibly constant for 0 2 pH units on either side of the control pH_o (usually 4 5). Proton absorption and potassium release accompanying glycine uptake were estimated by subtracting the extrapolated control traces (linear; see Fig 4) from the traces elicited by glycine. (When yeast cells are transferred from the stock suspension to fresh standard buffer medium, there is a sudden absorption of protons, amounting to 10–25 nequiv./mg dry wt cells, and an equivalent release of potassium ions (measurable only at low extracellular K^+ concentrations) The phenomenon is complete within 10–15 s, is independent of incubation temperature or metabolic status of the cells, is diminished by elevating either pH_o or $[K^+]_o$, and is presumed to represent cation exchange within the fixed-charge regime of the yeast cell wall. The experimental trace shown in Fig. 4B, and most data obtained in subsequent experiments, were taken after the initial burst, although a few observations (e g , Fig 4A) were corrected numerically.)

In several experiments for which simultaneous measurements of glycine uptake and H^+ or K^+ flux were required, 0.5-ml samples of suspension were withdrawn from the water-jacketed vessel at suitable intervals, harvested on Millipore filters (0 8 μm pore size), and processed and assayed for [^{14}C]glycine as described above.

Photometry and electrodes for K^+. Cytoplasmic potassium was determined by absorption photometry (Perkin-Elmer 360 Atomic Absorption Spectrophotometer) on the same water extracts (see above) prepared for the [^{14}C]glycine assays.

K^+-sensitive electrodes for the H^+/K^+-flux measurements were made by capping pulled capillary tubes (outer diameter 1 5–3 0 mm) with a valinomycin-impregnated polyvinylchloride membrane The internal reference half-cell for this K^+ electrode was Ag-AgCl in 0.1 M KCl

^{31}P-NMR experiments For the determination of intracellular pH by ^{31}P-NMR, cells were suspended in buffer at a density of 15–25 mg dry wt /ml NMR samples consisted of 15 ml of this suspension in a 20-mm (outer diameter) NMR tube, into which two bubblers were inserted During aerobic experiments, a mixture of 95% O_2/5% CO_2 was bubbled through the samples; and during anaerobic experiments, a mixture of 95% N_2/5% CO_2

The ^{31}P-NMR spectra were obtained at 145.78 MHz on a Bruker WH 360 WB NMR spectrometer The probe temperature was maintained at 30 °C during the experiments Spectra were accumulated in blocks of 15 or 30 s, using pulse intervals of 0 34 s, and 50° flip angles. Time-courses were followed for 15–30 minutes. For a chemical-shift standard, glycerophosphoryl choline (1–3 mM) was added to the suspension at the end of each experiment, its chemical shift, which is independent of pH, was set to 0.49 ppm (referenced to external 85% H_3PO_4 [27]. Intracellular pH was then determined from the chemical shift of intracellular orthophosphate

The same titration curve was used as previously (see below, Inset Fig. 5, Ref. 28) The end-points of that curve are 0 73 ppm (chemical shift at low pH) and 3 22 ppm (chemical shift at high pH), with a pK of 6.67 Although the pK of the titration curve is somewhat dependent on ionic strength [26], possible errors from this source were minimized in the experiments by calibrating the phosphate resonance in a medium of ionic strength similar to cytoplasm, and by holding the extracellular ionic strength constant throughout the experiments While residual uncertainty may affect absolute values of cytoplasmic pH estimates (conceivably by as much as 0 15 pH unit), there should be no effect on measured pH changes.

Results

General description of glycine transport in Saccharomyces

Accumulation by energy-starved cells For the study of coupled proton/amino acid transport in yeast, cells which have been energy-starved (for example, by treatment with 2-deoxyglucose and antimycin [12]) have proven most useful, since they clearly and reproducibly display the H^+ net fluxes, as well as the coupled amino acid (isotopic) fluxes [37,38]. Under certain conditions, energy starved yeast have been shown actually to accumulate glycine [12,15], and from submillimolar extracellular concentrations they can establish cy-

toplasmic steady-state levels very near those achieved by aerobic or simple anaerobic cells. This situation is demonstrated by the solid-line plots of Fig. 1A. Such data might suggest an energy-independent accumulation mechanism, such as intracellular binding or chemical conversion But closer inspection reveals that, at the suspension densities used in these experiments (approx. 15 mg dry weight per ml of buffer solution; selected to optimize the NMR signals), energy-starved cells could reduce extracellular glycine from the starting value of 0.4 mM only to about 80 μM, whereas aerobic cells could reduce the level to 5 μM (Fig. 1A, dashed-line plots) Thus accumulation ratios of about 10^2 in starved cells must be compared with ratios of 10^3 or greater [15] in aerobic cells (Fig. 1B) Furthermore, Eddy et al [12] have shown that glycine metabolism (chemical conversion) in energy-starved cells is negligible and that essentially all glycine transported is readily extracted into free solution, so it is not tightly bound in the cytoplasm Evidently, then, a residual energy supply for transport must exist in energy-starved cells. The normal transmembrane pH difference (approx 2 units, inwardly directed $pH_i \simeq 6.5$, $pH_o = 4.5$) is thermodynamically sufficient to drive the observed accumulation, and Eddy and his collaborators [12,15] used elevated pH_o (7 4) to suppress glycine accumulation by starved cells.

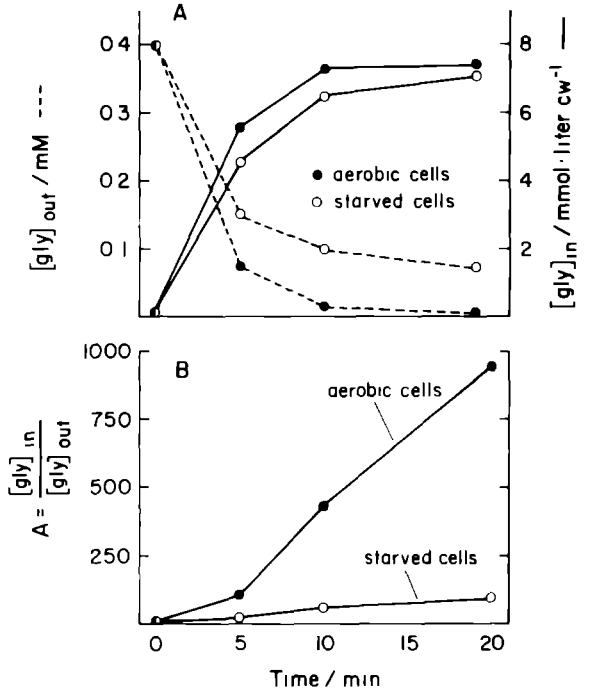

Fig 1 Glycine uptake by *Saccharomyces cerevisiae*, in aerobic (●) and energy-starved (○) states (A) Concentrations: solid lines indicate intracellular glycine, dashed lines, extracellular glycine (B) Calculated concentration ratios cytoplasm/medium. Cells were suspended at a density of 15 4 mg dry wt./ml, partitioned into 10-ml aliquots in 50-ml Erlenmeyer flasks, and shaken at 90 strokes/min, 30 °C. For starved cells, 2-deoxyglucose (5 mM) and antimycin A (0 5 μg/mg dry wt of cells) were added at −5 min. [^{14}C]Glycine (0 4 mM) was added at zero time. Medium in all cases was standard buffer medium (20 mM Tris citrate, pH 4 5) The cell water/dry weight ratio was assumed to be 2 4 [15].

Dependence of glycine influx upon extracellular pH. Both aerobic cells and energy-starved cells take up glycine via two separate carrier systems, although different laboratories and different yeast strains (i.e., *S cerevisiae* and *S carlsbergensis*) have given quite different kinetic parameters for the two systems [14,39]. Our own survey of pH_o effects on glycine influx from different extracellular concentrations has confirmed the existence of

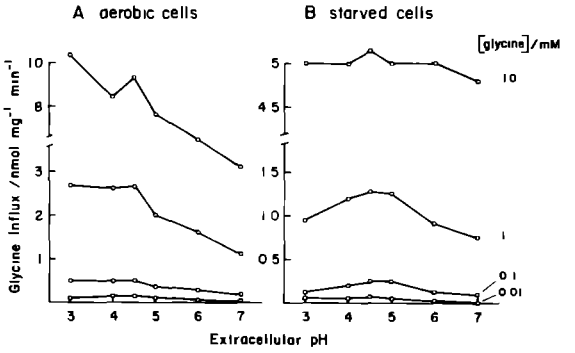

Fig 2. Survey of the effect of extracellular pH on glycine influx Conditions for aerobic (A) and starved cells (B), as described in Experimental Procedures and in Fig 1. Fluxes calculated from uptake in the first minute after addition of glycine Cell density in all trials 15 4–16 0 mg dry wt /ml suspension Values plotted have not been corrected for glycine depletion by transport. For pH 4 5, the required correction would be about 10% at 0.01 mM, 5% at 0.1 mM, and negligible at the higher glycine concentrations. Ordinate scale is given in nmol/mg dry wt of cells per min. (The absolute magnitudes of glycine flux in this experiment were about half the size expected from most of our other measurements on *S. cerevisiae* (see, Fig 9 for starved cells, 0.2 mM glycine) The origin of this variability is unknown)

two distinct transport systems, both of which are kinetically altered by energy starvation The primary fluxes, obtained as initial rate measurements (uptake in the first minute), are summarized in Fig 2 For aerobic cells, the plots show no distinct pH optimum, and glycine influx at all concentrations increases as extracellular $[H^+]$ is increased, at least to pH 3 In energy-starved cells, on the other hand, there appears to be a broad transport optimum around pH 4 5, though (in the absence of a detailed kinetic analysis) the data could be interpreted to show an approximate pH-independence of glycine influx.

By fitting a simple 2-carrier model to these data, and testing with fixed kinetic parameters for as many conditions as possible [39], we have found the glycine-binding affinities to be independent of pH_o and energetic status for both carriers, while the apparent maximal velocities are sensitive to pH_o and and energetic status Formally, a function of the type

$$J = \frac{{}^1J_{max}[S]}{{}^1K_{1/2} + [S]} + \frac{{}^2J_{max}[S]}{{}^2K_{1/2} + [S]} \quad (1)$$

describes all the plots, with ${}^1K_{1/2} = 13\,7 \pm 1.3$ mM, ${}^2K_{1/2} = 0.38 \pm 0.04$ mM, and the J_{max} values displayed in Fig 3 ${}^1J_{max}$, for the low-affinity system, is relatively insensitive to extracellular pH, particularly in starved cells, but ${}^2J_{max}$, for the high-affinity system, falls with rising pH_o, regardless of metabolic status

(It is to be expected the J_{max} values will be underestimated, and $K_{1/2}$ values overestimated, in the present experiments. Very high cell densities have been used, so that extracellular concentrations of glycine fall quickly with transport, particularly at the lower starting concentrations (see Fig. 2) Therefore, the value of 0.38 mM for the high-affinity $K_{1/2}$ should be taken as an upper limit; such depletion may account for the discrepancy in comparison with $K_{1/2} = 0.15$ mM, as reported by Kotyk and Rihova [39] but not with 0 06 mM, stated by Eddy and Nowacki [14] For the remainder of experiments to be described below, the precise value of ${}^2K_{1/2}$ is not important, all experiments were carried out at a glycine concentration (0 2 mM) where the observed flux could be attributed 80% or more to the high-affinity system.)

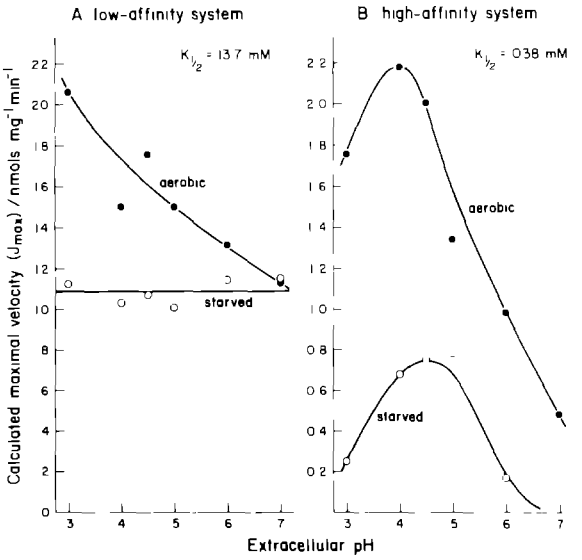

Fig 3 Apparent maximal velocities for glycine transport, as functions of extracellular pH (A) Low-affinity system (B) High-affinity system Data from Fig 3 were fitted to Equation 1 by means of a non-linear least-squares algorithm (Marquardt, 1963) Apparent Michaelis constants for both low- and high-affinity transport systems were independent of pH and metabolic status, with values of ${}^1K_{1/2} = 13\,7 \pm 1\,5$ mM and ${}^2K_{1/2} = 0\,38 \pm 0\,05$ mM The solid curves shown have been drawn by eye

Stoichiometric flux of protons and potassium The simplest and most widely accepted way to estimate the stoichiometry of ion-coupling to nutrient cotransport systems is to measure the initial changes of pH_o and $[K^+]_o$ upon addition of the substrate to previously non-transporting cells Typical experiments, using extracellular K^+- and pH-sensitive electrodes with both aerobic and energy-starved yeast cells, are shown in Fig 4 In part A, cells were added to air-bubbled standard buffer medium containing 1 mM KCl, and a steady-state acidification (upper trace) was observed at about 1 nequiv. H^+/mg dry wt per min (range, 1–3), along with a smaller uptake of K^+ When 0.2 mM glycine was added to the suspension, no change in either the H^+- or the K^+-trace could be detected. In part B, however, addition of 2-deoxyglucose + antimycin (prior to glycine) inverted both control traces, revealing a steady net influx of protons and efflux of K^+. (For the whole set of 16 experiments of this type which were carried out, the apparent stoichiometry of H^+/K^+

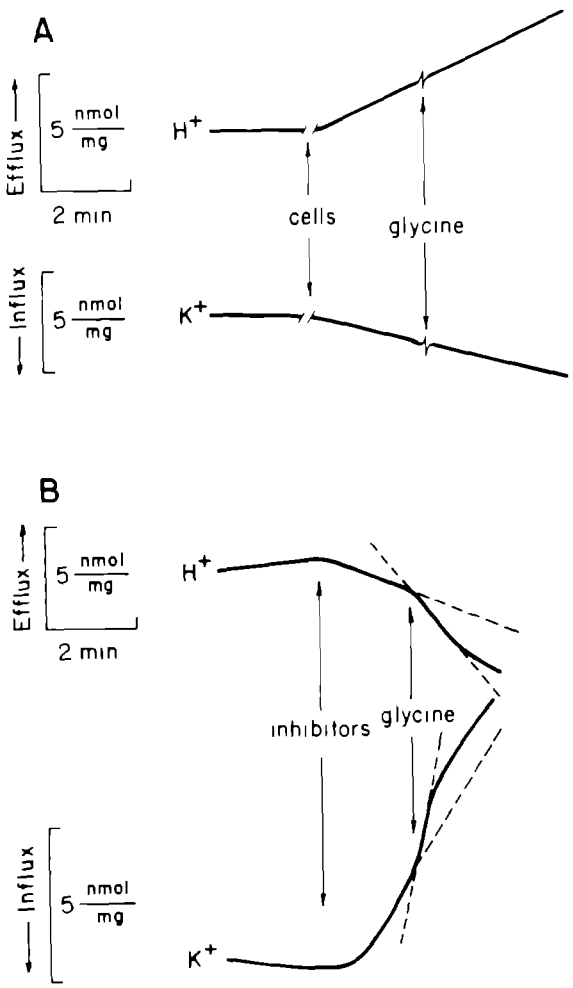

Fig 4 Proton and potassium fluxes accompanying glycine transport (A) Air-bubbled standard buffer medium containing 1 mM KCl, cells added (density of 20 5 mg dry wt /ml) during the gap in the traces, steady H^+ efflux and K^+ influx: 1 and 0 5 nmol/mg dry wt per min, respectively (B) Conditions as in (A), but cells were introduced 10 min prior to the trace shown, and 2-deoxyglucose (5 mM) and antimycin (0.25 μg/mg dry wt) were added at the first arrow Test glycine concentration in both cases was 0 4 mM

flux during brief 'starvation' was 0 9, treatment for half an hour could reduce $[K^+]_i$ from 160 to about 110 mequiv./liter cell water) And subsequent addition of glycine further stimulated the ion fluxes for a period of 1–2 min From the slope differences (between dashed lines) just before and after glycine addition, the initial net fluxes were calculated to be $1\ 61 \pm 0.15$ nequiv /mg dry wt. per min for H^+, and $1.25 \pm 0\ 18$ for K^+ Measurement of [^{14}C]glycine uptake in parallel experiments gave influxes of $1.66 \pm 0\ 18$ nmol/mg dry wt. per min, for an apparent proton . glycine stoichiometry of $0\ 97 \pm 0\ 14$ Thus, if we assume integral stoichiometries for H^+-glycine cotransport and for charge compensation by K^+ exit, then the ratio H^+ glycine · K^+ of 1 . 1 . 1 is most reasonable.

This finding clearly differs from the ratio 2 : 1 : 2 deduced for *S carlsbergensis* [14,37,38], but is consistent with the general observation that apparent proton· amino acid stoichiometries between 1 and 3 occur in different yeast strains or in the same strain grown under different conditions The issue of 'real' versus apparent stoichiometries in cotransport systems will be taken up explicitly in the Discussion

Response of intracellular pH to glycine transport

Our initial objectives in studying intracellular pH during glycine transport were first, to verify the glycine-coupled proton flux which had been postulated on the basis of extracellular pH changes (e.g , Fig 4B), and second, to redetermine the H^+ glycine stoichiometry. Intracellular pH was calculated from the NMR chemical shift for intracellular inorganic phosphate, as shown in Fig. 5 A typical ^{31}P-NMR spectrum for aerobic yeast cells is given in the upper trace, it reveals a major peak for orthophosphate ($P_{i(c)}$) and four for polyphosphate (PP_1, PP_2, PP_3, PP_4), as well as minor peaks for sugar phosphate (S-P), pyridine nucleotide, nucleoside triphosphatase, and a small second peak for orthophosphate ($P_{i(v)}$). The larger peak for orthophosphate, along with the consequent computed pH_i, has been assigned to the bulk cytoplasm [27]. The smaller orthophosphate peak has been assigned to the yeast vacuole [26], and can vary both in size and chemical shift, depending on metabolic conditions (see discussions in Refs. 26, 31 and 32). During energy starvation, the nucleoside triphosphate peaks nearly disappeared (lower trace in Fig 5), the peak for orthophosphate declined slightly, but mainly shifted upfield, and the sugar-phosphate peak shifted downfield and increased greatly, probably because of accumulating non-metabolizable 2-deoxyglucose 6-phosphate

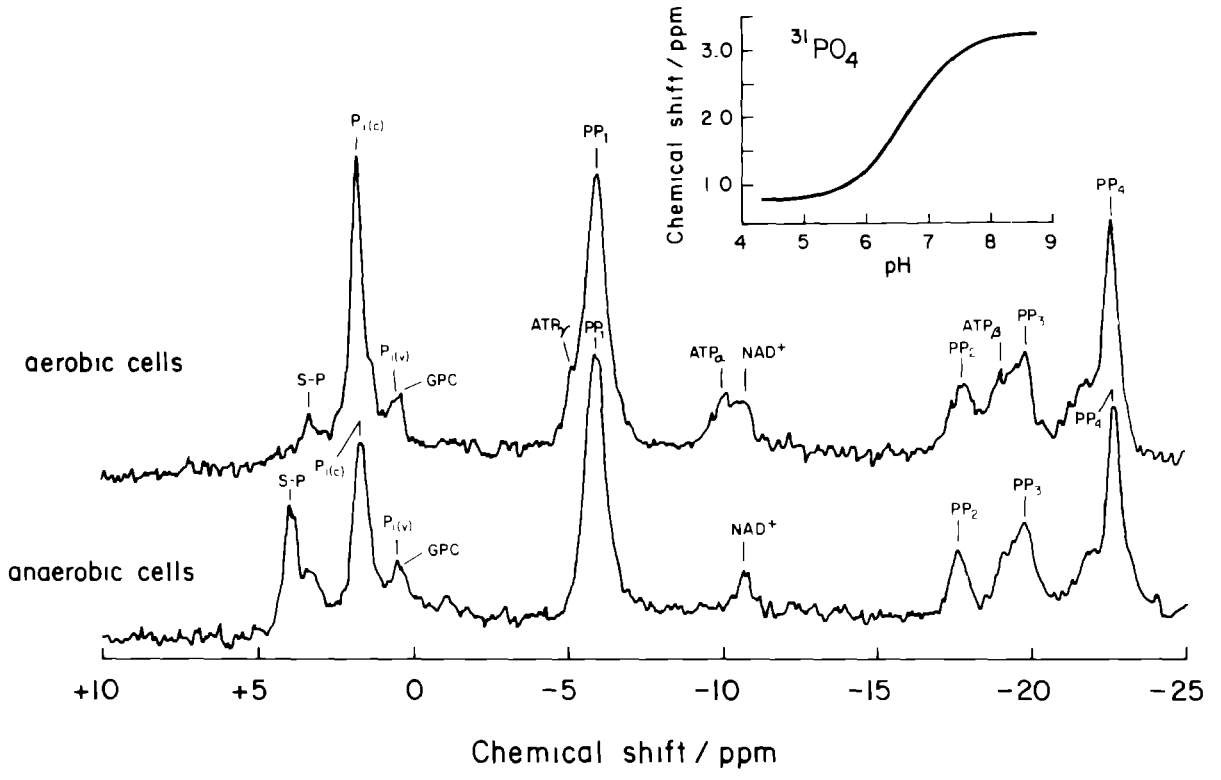

Fig 5 ^{31}P-NMR spectra of aerobic and anaerobic yeast Aerobic cells 22 5 mg dry wt cells/ml, in standard buffer medium bubbled with 95% O_2/5% CO_2 at 50 ml/min Anaerobic cells Same suspension bubbled for 20 min with 95% N_2/5% CO_2 Symbols $P_{i(c)}$ = cytoplasmic orthophosphate; $P_{i(v)}$ = vacuolar orthophosphate, PP_1, PP_2, PP_3, PP_4 = shifts for different residues in polyphosphate, S-P = sugar phosphate, NAD^+ = pyridine nucleotide, ATP_a, ATP_b, ATP_g = shifts for the three phosphate residues in adenosine triphosphate, GPC = glycerophosphorylcholine, added as an internal calibrating standard (chemical shift at 0.49 ppm, independent of pH) Tracings represent spectra accumulated for 5 min Inset. Standard curve for the resonance shift of orthophosphate with pH, adapted from Den Hollander et al [28].

pH_i for aerobic cells (bubbled with 95% O_2/5% CO_2) ranged from 7.2 to 7.4 in all experiments, and for sustained anaerobic (bubbled with 95% N_2/5% CO_2) or energy-starved cells ranged from 6 6 to 6.9. Cytoplasmic acidification occurred slowly, either with anoxia or with energy starvation (addition of 2-deoxyglucose and antimycin to previously aerobic cells); in the former case it was linear at 0.02 pH/min, and in the latter case it was exponential, with a half-time of 6–7 min (see Fig 7 below, for details). Extracellular pH per se had no measurable effect on intracellular pH, either in aerobic cells or starved cells, reconfirming the earlier finding of Salhany et al. (1975)

Because intracellular pH stabilizes rather slowly during energy starvation or anoxia, it was necessary as a practical matter to examine possible transport-linked changes of pH_i against a shifting baseline. Plotted time-courses of pH_i, before and after addition of 0.2 mM glycine to starved cells, are shown in Fig. 6. The intrinsic scatter of the NMR measurements was about 0.03 pH unit, so it was necessary to calculate regression slopes in order to quantify the effect of glycine. The difference in slopes between plot A and plot B (after glycine) amounts to a cytoplasmic pH change of 0 011 unit/min. The example in Fig. 6 has been selected as a 'typical' result. A total of 19 experiments of this type were conducted, and the average slope difference was 0.005 pH units/min, acidification; but, as shown in Table I (column 4), individual values ranged from −0.060 to +0.074. Scatter was magnified somewhat by variability in the control values of pH_i (Table I, column 1), but

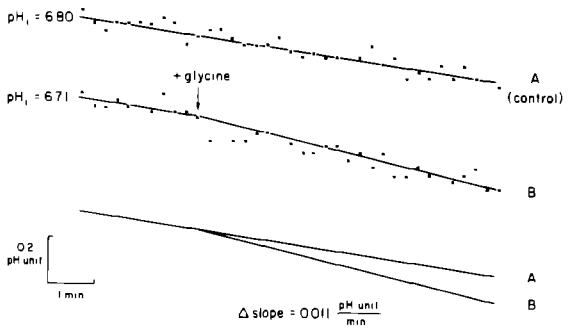

Fig 6 Time-course of pH_i in starved cells before and after addition of 0 2 mM glycine. (A) Control (cells treated with deoxyglucose and antimycin 6 min before beginning of the plot) (B) Same conditions as in A, exactly parallel experiment, but 0 2 mM glycine added at the arrow Cell density in both cases 21 4 mg dry wt./ml standard buffer medium Regression lines were fitted with a common slope for all points in plot A plus points prior to glycine in plot B [40]

that effect was minimized by introducing cytoplasmic buffer capacity for calculation of actual proton fluxes

Cytoplasmic buffer capacity in *S cerevisiae* was determined by forcing changes of pH_i with extracellular addition if permeant acid or base (butyric acid or procaine) The method has been adapted from the measurements of Sanders and Slayman [24] on *Neurospora crassa*, and will be detailed for yeast in a separate paper (Ballarin-Denti et al., in preparation). The pertinent values for present purposes are listed in Table I, column 5. Actual proton fluxes associated with glycine uptake have been calculated as the product of the slope difference and buffer capacity, adjusted for the ratio of cell water · dry weight (2.40), and are displayed in Table I, column 6. The mean value of 1.20 nmol H^+/mg dry wt. per min should be

TABLE I

CYTOPLASMIC PROTON FLUXES ASSOCIATED WITH GLYCINE UPTAKE IN *S CEREVISIAE*

pH at zero time	Control [a] slope (pH/min)	Slope after glycine (pH/min)	Δ slope [b] (ΔpH/min)	Buffer [c] capacity (β)	Glycine stimulated influx [d]
6 05	0 0470	0 0499	0 0028	202	1 44
6 27	0.0107	0 0115	0 0007	131	0 24
6 72	0 0378	0 0327	−0 0050	50	−0 62
6.57	0 0290	0 0330	0 0040	69	0 70
6.53	0 0077	0 0275	0 0190	75	3 56
6.71	0 0046	0.0173	0 0127	51	1 58
6 64	0.0160	0.0204	0 0044	60	0 66
6 59	0.0134	0 0093	−0 0040	66	−0 65
6 48	0 0068	0 0554	0 0480	85	10 20
6 48	0 0075	0.0109	0 0039	85	0 72
6 45	0 0226	0.0176	−0 0050	90	−1 12
6 79	0 0655	0 0631	−0.0024	43	−0.27
6 72	0 0174	0 0000	−0.0174	50	−2 18
6 76	0.0474	0.0460	−0 0013	46	−0 14
7.03	0 0920	0 0320	−0 0600	25	−3 75
6.88	0 0128	0 0075	−0.0053	35	−0 46
6.75	0.0091	0.0215	0 0124	47	1 39
6 68	0.0690	0 1430	0 0740	55	10 18
6 70	0 0206	0 0306	0 0099	53	1 36
				Average	1 20 ± 0 78

[a] Slopes and Δslopes were obtained as described in the legend of Fig. 6, for energy-starved cells suspended in standard buffer medium.

[b] Negative slopes indicate alkalinization of the cytoplasm

[c] Buffer capacities were read from a standard curve obtained by measuring the effect of extracellular butyric acid and/or procaine (at known concentrations) on cytoplasmic pH Unit mmol H^+/liter cell water per pH unit

[d] The average Δflux is given ± 1 S E. Unit: nmol H^+/mg dry weight per min

compared with a glycine flux of 1.66 nmol/mg dry wt per min from the experiments with ΔpH_o, to yield an apparent H^+ · glycine stoichiometry of 0 72. This result again is consistent with an integral stoichiometry of 1 1, but scatter in the measurements clearly makes the argument a weak one Similar experiments conducted on aerobic cells (data not shown) gave no detectable change of pH_i on addition of glycine, despite the 2- to 3-fold faster glycine flux (see Fig 2)

Behavior of pH_i and glycine flux with metabolic inhibition

Because of a prior observation concerning the effects of metabolic inhibitors on glycine transport (presented below), we decided to examine the time course of changing intracellular pH with different inhibitors. Experiments were conducted on the pattern of Fig. 6, except that the inhibitors, rather than glycine, were added at the arrow in plot B, and NMR readings were taken for 15 min thereafter. Summary plots of the results are shown in Fig. 7, from which two categories of inhibitors can be discerned: (i) those dropping pH_i to the range (6.6–6 9) characteristic of anoxia antimycin + deoxyglucose, cyanide, dicyclohexylcarbodiimide (DCCD); and (ii) those producing a much larger and more rapid acidification, taking pH_i from the control value down to about pH 6 within 5 min two presumed protonophores, azide (KN_3) and 2,4-dinitrophenol (DNP)

Evidently, metabolic events which govern intracellular pH are similar whether blockade occurs in respiration (N_2, KCN), in respiration plus glycolysis (deoxyglucose + antimycin), or in the mitochondrial and plasma-membrane ATPases (DCCD) But another event supercedes with azide or 2,4-dinitrophenol. It is not known for certain whether this event involves influx of extracellular protons, massive proton loss from the vacuoles, or shifted synthesis of organic acids

More important for the moment is the fact that the effectiveness of various agents in causing cytoplasmic acidification in *S. cerevisiae* appears directly related to their efficacy as transport inhibitors Fig 8 shows uptake of glycine by yeast maintained either aerobic (A) or energy starved (B), and with the designated inhibitor added 5 min before [^{14}C]glycine Comparison of Figs 7 and 8 reveals that glycine influx and pH_i fall approximately in parallel, with the different inhibitors (except in the case of DCCD added to starved cells) The moderate or intermediate level of inhibition observed in simple energy-starved cells is

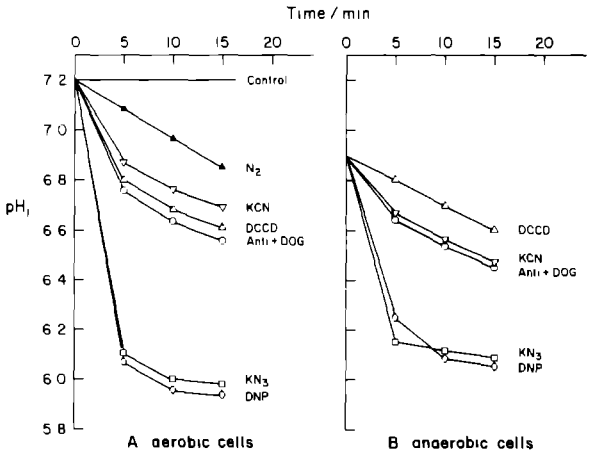

Fig 7 Influence of various metabolic inhibitors on cytoplasmic pH of yeast Experiments conducted as in Fig 6, with each inhibitor added several minutes after commencement of NMR recording Cell density 23 7 mg dry wt /ml standard buffer medium; inhibitor concentrations N_2, 0 95 atm (+0 05 atm CO_2), antimycin A, 0 25 μg/mg dry wt cells, deoxyglucose (DOG), 5 mM, KCN, 1 mM, dicyclohexylcarbodiimide (DCCD), 5 mM KN_3, 1 mM, 2,4-dinitrophenol (DNP), 0 2 mM.

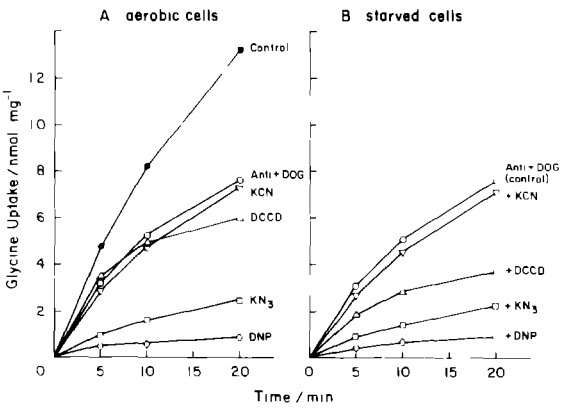

Fig 8 Influence of different metabolic inhibitors on glycine uptake Experiment conducted as in Fig 1, but with each inhibitor added 4–5 min before [^{14}C]glycine Deoxyglucose and antimycin were present in all experiments with starved cells Cell density 24.7 mg dry wt /ml Inhibitor concentrations as in Fig. 7

in fact a key 'permissive' feature of the experimental conditions originally devised by Eddy and his collaborators, and adopted for many of the present experiments

Dependence of glycine flux upon pH_i, pH_o, and ΔpH

A third fact which emerges from comparison of Figs 7 and 8, is that the apparent dependence of glycine influx upon intracellular pH can be steep, especially so in anaerobic/starved cells· for 2,4-dinitrophenol versus the control (antimycin + deoxyglucose), a 2 8-fold increase of $[H^+]_i$ (0.44 pH_i difference) is associated with a 7.5-fold decrease of flux. The simplest way to account for such steepness would be to suppose that binding and release of two or more protons are associated with the uptake of a single glycine molecule The observation itself may be compromised by other effects of the inhibitors (e g , on metabolism or membrane potential), and a more direct study of the pH_i-effect on glycine influx was required, because the supposed 2 1 stoichiometry would directly conflict with the 1 1 stoichiometry obtained (see Fig. 4 above) from extracellular proton removal

A method for systematically changing intracellular pH, while monitoring it via ^{31}P-NMR, has already been alluded to in connection with Table I and the buffer capacity measurements· to add extracellular weak acids or bases (butyrate, procaine). Measurement of glycine fluxes in parallel trials then gives a correspondence between forced pH_i and transport. Such experiments have been carried out on starved cells, in order to be strictly comparable with the proton flux measurements Results for one set of experiments are plotted in Fig 9A. filled symbols represent the flux itself (left ordinate scale), plotted against pH_i, and open symbols represent the Hill function for flux, plotted on a log scale (right ordinate) against pH_i. From the steepest portion of the linear plot, flux increases at a rate of $J_{max}/0\,5$ pH units (the extrapolated value of J_{max} is 0.75 nmol/mg per min for these experiments), which compares with a theoretical maximum for single-charge carrier transport of $J_{max}/0.87$ pH unit [35]. The overall slope on the log-log (Hill) plot is 3 0. These results appear to confirm the above suggestion that up-

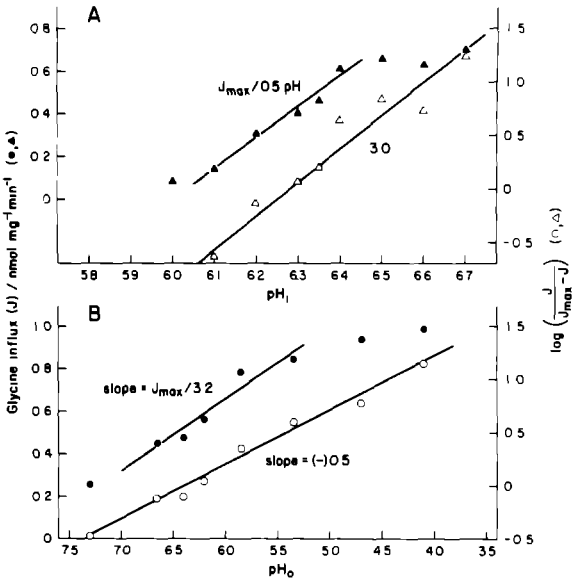

Fig 9 pH-dependence of glycine influx (A) Varied intracellular pH, with $pH_o = 5\,7$. (B) Varied extracellular pH, with $pH_i = 6\,7$ Filled symbols Flux versus pH (left ordinate scales) Open symbols Hill plots (right ordinate scales) Straight lines are least-squares fits for the points included, with slope values shown, J_{max} assumed equal to 0 75 and 1 06 nmol/mg dry wt per min, respectively, for A and B General conditions as in Fig 1, with extracellular glycine = 0 2 mM Cell densities were 12 5 mg dry wt /ml in A, 13 9 mg dry wt /ml in B The following table gives the total concentrations (mM) of butyrate (titrated to pH 5 7), which were necessary to reduce intracellular pH to the values plotted

pH_i	6 0	6 05	6 1	6 2	6 3
Butyrate	54 6	41 7	32 0	18 7	10 0
pH_i	6 35	6 4	6 5	6 6	6 7
Butyrate	7.2	5 1	2.4	0 8	0

take of each glycine molecule is associated with binding and dissociation of more than a single proton

An important methodological check for this conclusion is to examine glycine flux in a similar fashion with changes of extracellular pH. Results from such a series of experiments are plotted in Fig. 9B. In this case the maximal slopes are $J_{max}/3.2$ pH unit and 0 5, respectively, for the linear and log-log plots, which again conflict with the measured stoichiometry of 1 · 1, since, taken simply, the data would imply cotransport of only

0 5 proton per glycine molecule. The high-affinity glycine transport system in yeast thus appears surprisingly insensitive to the extracellular concentration of its cosubstrate, H^+. Obviously, any kinetic scheme which purports to describe glycine transport in *S cerevisiae* must first of all reconcile three very different estimates of H^+ : glycine stoichiometry· 1 1 from net proton fluxes; 2, 3 1 from pH_i sensitivity, and 0 5 from pH_o sensitivity.

A simple class of carrier models suitable for this purpose is presented in the Discussion

Discussion

A kinetic model

General considerations of cyclic reaction schemes for cotransport [20,41] indicate that a simple, single-loop carrier with ordered binding can accommodate most of the data reported here on H^+-glycine cotransport in *S cerevisiae*, provided that suitable restrictions are placed on the sequential reaction constants Trial calculations have led to the specific scheme shown in Fig. 10A,

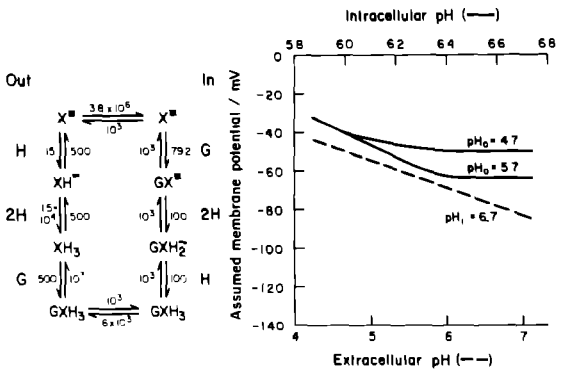

Fig 10 Reaction scheme for an ordered kinetic model which describes high-affinity glycine transport in energy-starved yeast Left half-figure Reaction diagram Right half-figure pH-dependence of membrane potential required to fit the model to glycine flux data (Features of this model which are essential, either as starting assumptions or as properties emerging from the data, are outlined in the Discussion Arbitrary properties built in for convenience are the following (i) The fully loaded carrier is neutral, and the unloaded carrier is negative (ii) For the bimolecular steps, indicated reaction constants implicitly contain the ligand concentrations, and all reaction constants contain a common scaling factor for site density and turnover number The numerical values given incorporate $5.6 \cdot 10^7$ turnovers/cm^2 per s, $[glycine]_o = 0\,2$ mM, $[glycine]_i = 1$ mM [15], $pH_o = 7$, $pH_i = 6\,7$)

which assumes (as is usual for cotransport systems) that total carrier is conserved, that measurements are made under steady-state conditions, and that gradient energy alone drives the system (meaning the clockwise/counterclockwise ratio of rate products must equal the corresponding ratio of ligand products) Salient features of the model which fit it to Figs. 3, 6, and 9 are the following.

(1) Three hydrogen ions are bound and released during each cycle ($z = 3$), and the three binding sites dissociate at similar cytoplasmic pH values below the physiological range ($pK_{1i} = 5.7$).

(2) Membrane potential, which can be incorporated in the form of a symmetric Eyring barrier (rate constants for transit of the fully loaded carrier assumed proportional to $\exp(\pm zF\Delta\psi/2RT)$; [35,42]), is pH-dependent to the extent shown in Fig 10B (solid curves: pH_i; dashed line: pH_o)

In modelling the pH_i-dependence of transport, a trade-off occurs between the proton stoichiometry and the pH-slope of membrane potential We have chosen three protons per cycle as a reasonable stoichiometry which also gives a palatably small effect of pH on $\Delta\psi$; but two or four protons per cycle (with correspondingly steeper or shallower pH-dependence of $\Delta\psi$) would also fit the data. No reliable methods have yet been devised to measure $\Delta\psi$ in yeast (for critique, see Borst-Pauwels [43]), but the range and pH_o-sensitivity of potential indicated in Fig. 10B are compatible with steady-state electrophysiological data from cyanide-inhibited *Neurospora* (Slayman, C L , unpublished experiments)

(3) The low sensitivity of glycine flux to pH_o (Fig. 9B) requires that two of the external proton-binding sites be saturated over the pH range studied, so that only a single proton appears to be reacting. Thus, only pK_{1o} (= 5 5), for the first extracellular binding site, is much affected by the normal acidic extracellular pH values

(4) To obtain a predominant J_{max} effect of extracellular pH (Fig. 3), extracellular glycine needs to be bound after the protons are bound, in an ordered reaction As the model stands, it yields about a 7-fold decrease of J_{max} and a 3-fold decrease of $K_{1/2}$, for the shift of pH_o from 4 0 to 7 0.

Fig 11 shows glycine flux curves, calculated from the model of Fig. 10 and superimposed on the data of Fig. 9, plus an additional flux curve

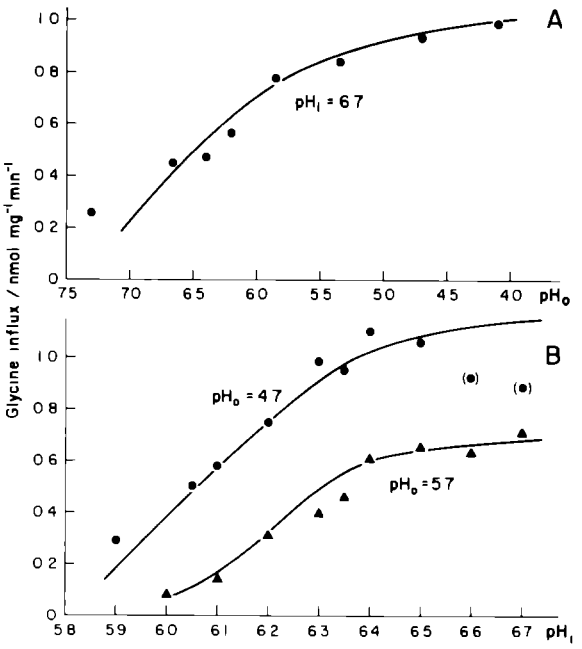

Fig 11 Fit of observed glycine fluxes by the reaction kinetic model of Fig 10 (A) pH_o, from Fig 9B, (B) pH_i, from Fig 9A (lower curve), and from a similar experiment with $pH_o = 4\,7$ (upper curve) (Each of the three data plots represents a separate glycine flux experiment, and the variability of fluxes from one experiment to the next (legend Fig 2) necessitated a slight scaling of absolute flux values in order to fit all three data sets with the model of Fig 10 Scaling factors used were 1 0, 1 20, and 0 85, in order from top to bottom)

obtained by varying internal pH at a fixed extracellular pH of 4.7 (upper plot, Fig 11B). The fits have not been statistically optimized, since their purpose is not to establish parameter values, but rather to demonstrate the general applicability of this kind of model and to point out the constraints which the data demand The apparent inhibition of glycine flux which sometimes occurs above $pH_i = 6\,5$ (upper plot, Fig. 11B) cannot be accommodated by the model of Fig. 10, and those two points have been excluded from the fit calculations.

Membrane potential and measured proton stoichiometry

While at first sight it may seem unreasonable to invoke a role for membrane potential in energy-starved cells (which have been largely depleted of cytoplasmic ATP [12]), there are three important reasons for doing so, quite apart from expedience in manipulating the kinetic model The primary reason is that even in the total absence of active transport, passive ion systems in the membrane will respond to any imposed membrane potential or change thereof. The second reason is that in a fungus such as *Neurospora*, where direct measurements of $\Delta\psi$ can be made, it is virtually impossible to abolish membrane potential by energy-starvation or anoxia. Acute treatments with deoxyglucose or cyanide (plus salicylhydroxamic acid, to block cyanide insensitive respiration) quickly depolarize the membrane (from a normal value of approx $(-)200$ mV), but only to the range -30 to -50 mV. Despite the simultaneous drop of cytoplasmic ATP concentration to approx. 10% [44,45], almost any kind of metabolic downshift 'tightens' the *Neurospora* membrane so that smaller ionic currents can generate substantial membrane potentials [46] And the third reason comes from the K^+-dependence of H^+-glycine cotransport in yeast· cytoplasmic K^+ is required, while extracellular K^+ is a non-competitive inhibitor [12,14] Though these facts might implicate K^+ as a reaction cofactor, it is at least as simple to imagine that a K^+ diffusion potential accelerates H^+-glycine cotransport. It is a satisfying confirmation, therefore, that the model of Fig. 10 (with reaction constants as shown) predicts that membrane depolarization should act like a non-competitive inhibitor of glycine transport.

Now, in order to reconcile a 3-H^+ model with smaller measured stoichiometries (1 : 1 presently in *S. cerevisiae*, and in Eddy's measurements on *Candida utilis* [47], 2 . 1 previously in *S carlsbergensis* and *S. cerevisiae* [14,37]), it is only necessary to consider how electroneutrality must be maintained during glycine-coupled proton influx. Because the membrane must depolarize somewhat under this proton flux, movements of all other permeant ions must also change: K^+, cytoplasmic organic anions, and (especially important in 'chemiosmotic' systems like the yeast plasma membrane) H^+. Electroneutrality will be maintained, after the recharging of membrane capacitance (< 100 ms), by reduced K^+ influx, by increased anion efflux, and by reduced proton influx via pathways other than the glycine systems. Thus, because of 'circuit compensation' in a proton-per-

meable membrane system, only a fraction of the unidirectional proton flux occurring via specific cotransport can be measured as net flux. It is tempting to conclude, therefore, that the principal reason for wide variation of H^+·amino acid stoichiometry, in different yeasts under different conditions, is variability in the background proton permeability of the membranes, rather than true variability in the cotransport coupling

The only basic remedy for this kind of error is to clamp the membrane potential. This can be done electrophysiologically, so the return current flows through an amplifier and can be compared directly with substrate flux (see Sanders et al [48] on the general amino acid transport system in *Neurospora*). Or, it can be done with lipid ionophores, such as valinomycin and gramicidin, as recently used to demonstrate 2.1 stoichiometry for Na^+-sugar transport in guinea pig intestine [49].

Cytoplasmic pH and the action of inhibitors

There has been a strong tendency, in the literature on proton-coupled transport systems, to interpret the inhibitory effects of uncoupling agents (such as dinitrophenol or carbonylcyanide *m*-chlorophenyl hydrazone (CCCP)) as resulting from abolition of proton gradients by dissipative proton conduction Under well-controlled conditions this interpretation may be correct, but for intact eukaryotic microorganisms other factors become important

The effect of 2,4-dinitrophenol (and of another presumed proton conductor, N_3^- (azide)) on glycine transport in yeast is an interesting case in point Eddy et al. [12] observed that while treatment with deoxyglucose and antimycin reduced initial glycine influx at low pH less than 2-fold in *S carlsbergensis*, added 2,4-dinitrophenol (0 2 mM) was much more effective, reducing the flux by 10-fold [15]. Data presented in Figs 7 and 8 above, however, make clear that transport inhibition is not accompanied by proton equilibration across the yeast cell membrane In the face of an external pH of approx. 4.5 (set by the Tris-citrate buffer), 0.2 mM 2,4-dinitrophenol lowers pH_i to approx. 6 0 leaving a residual pH difference equivalent to about +95 mV Since the resultant decline of chemical driving force on protons is only 25–40% (from control pH_i values of 6 7–7.2), the thermodynamic effect on protons simply cannot account for a 10-fold change in H^+-coupled glycine flux By contrast, the steep kinetic dependence of glycine flux upon pH_i (Fig. 9A) is more than sufficient to account for inhibition of glycine transport by uncouplers, both in the present experiments (Fig 8) and in all previous experiments

Since protons do not equilibrate across the yeast plasma membrane during strong metabolic inhibition or uncoupling, the source of protons for cytoplasmic acidification is open to question The amount of acid involved is considerable about 85 mmol/kg cell water, for acidification from pH 6 8 to 6 0 Considering the initial 5-min period, an average apparent influx of 30 pmol/s for each cm^2 of membrane (18 mmol/kg cell water per min in cells 6 μm in diameter) occurs with 2,4-dinitrophenol or KN_3 treatment of aerobic cells; initial influxes with the other inhibitors are about 10 pmol/cm^2 per s However, for energy starving cells (antimycin + deoxyglucose) the initial influxes estimated from alkalinization of the medium never exceeded 2 pmol/cm^2 per s (actually 0 6 pmol/cm^2 per s in the example of Fig 4B (upper trace, between the arrows).

This kind of mismatch between fluxes calculated from changes of internal pH and changes of external pH forces us to consider intracellular sources for a significant portion of the cytoplasmic H^+ load There are at least two such possible sources.

(1) The yeast vacuole, where inorganic phosphate and polyphosphate are stored, along with basic amino acids. Although the latter should not change ionization over the pH range 6 8 to 6 0, phosphate residues would do so These may be present at a total concentration of 1 M in the vacuole [50,51,52], with a relevant pK (pK_3 in pyrophosphate) near 5 8 Since vacuoles account for about 25% of yeast cell volume [50], they could yield about 330 mM of phosphate residues to the cytoplasmic volume Normal vacuolar pH can also be estimated near 5.8, from $P_{i(v)}$ in Fig. 5; and (given the cytoplasmic buffer curve of Table I plus the pK_3-buffer curve for polyphosphate) cytoplasmic pH could be lowered from 6.8 to 6.1–6.2 by total release of vacuolar polyphosphate or its acid equivalents. However, even though the effects

of specific inhibitors or uncouplers on vacuolar contents have not been explored in detail, total release in vivo within 5–10 min (Fig. 7) seems improbable. Vacuoles survive standard preparative procedures involving much longer periods of metabolic deprivation [50,51], furthermore, the spectra of Fig. 5 above show no major change in the chemical shifts of polyphosphate during sustained anoxia.

(ii) Catabolic reactions in carbon metabolism. Fungi in general (and *S. cerevisiae* in particular) are known to release substantial quantities of acid during either respiratory or glycolytic oxidation Sigler et al. [53] calculated H^+ efflux to be near 30 pmol/cm^2 per s for aerobic yeast suddenly given glucose ($pH_o = 4.5$); and their data also permit an estimate of 10–15 pmol/cm^2 per s for anaerobic yeast given glucose. With such large background fluxes, an uncoordinated downshift of energy metabolism by an inhibitor (e.g., shutting off acid release ahead of acid production) could produce apparent cytoplasmic acidification of the magnitude indicated in Fig. 7 Unfortunately for this kind of arithmetic, however, large background effluxes do not occur in starved cells. Indeed, as originally found by Eddy and his collaborators [14,37], starved cells show a steady net proton influx, in the neighborhood of 5 pmol/cm^2 per s (see Fig. 6 and Table I above) Thus, neither of the putative intracellular sources of H^+ seems adequate over the range of present experiments

Perhaps the most reasonable position to take at present, therefore, is that all three proton sources the medium, the vacuoles, and metabolic shifts can contribute to inhibitor-induced cytoplasmic acidification; but that the proportions of the three can vary with conditions

Acknowledgements

The authors are indebted to Professor R.G. Shulman for encouragement and stimulating discussion. The work was supported by N.I H. Research Grants AM27121 (to R.G S.), GM-15761, and GM-15858; and by a Fogarty Fellowship to A.B.-D.

References

1 Mitchell, P (1963) Biochem Soc Symp 22, 142–168
2 West, I C (1970) Biochem Biophys Res Commun 41, 655–661
3 Kaczorowski, G J and Kaback, H R (1979) Biochemistry 18, 3691–3697
4 Eddy, A A (1982) Adv Microb Physiol 23, 11–76
5 Luttge, U , Jung, K.-D and Ullrich-Eberius, C I (1981) Z Pflanzenphysiol 102, 117–125
6 Slayman, C L and Slayman, C W (1974) Proc Natl Acad Sci USA 71, 1935–1939
7 Komor, E and Tanner, W (1974) Eur. J Biochem. 44, 219–223
8 Komor, E (1977) Planta 137, 119–131
9 Komor, E , Rotter, M and Tanner, W (1977) Plant Sci Lett 9, 153–162
10 Racusen, R H and Galston, A W. (1977) Planta 136, 57–62
11 Kinraide, T.B and Etherton, B (1980) Plant Physiol 65, 1085–1089
12 Eddy, A A , Backen, K and Watson, G (1970) Biochem J 120, 853–858
13 Komor, E., Haass, D , Komor, B and Tanner, W (1973) Eur J Biochem 39, 193–200
14 Eddy, A A and Nowacki, J A (1971) Biochem J 122, 701–711
15 Seaston, A , Carr, G and Eddy, A A (1976) Biochem J. 154, 669–676
16 Serrano, R. (1978) Mol Cell Biochem 22, 51–63
17 Goffeau, A and Slayman, C W (1981) Biochim Biophys Acta 639, 197–223
18 Komor, E , Schwab, W G W and Tanner, W (1979) Biochim Biophys Acta 555, 524–530
19 Sanders, D and Hansen, U -P (1981) J Membrane Biol 58, 139–153
20 Sanders, D , Hansen, U.-P , Gradmann, D and Slayman, C L (1984) J Membrane Biol 77, 123–152
21 Walker, N A and Smith, F A (1975) Plant Sci Lett 4, 125–132
22 Kashket, E R and Wong, P T (1969) Biochim Biophys Acta 193, 212–214
23 Spanswick, R.M and Miller, A G (1977) Plant Physiol 59, 664–666
24 Sanders, D and Slayman, C.L. (1982) J Gen Physiol 80, 377–402
25 Shulman, R G , Brown, T R , Ugurbil, K Ogawa, S , Cohen S M and Den Hollander, J A (1979) Science 205, 106–166
26 Gillies, R J., Alger, J R , Den Hollander, J.A and Shulman, R G (1982) in Intracellular pH Its Measurement, Regulation, and Utilization in Cellular Function (Nuccitelli, R and Deamer, D , eds), pp 79–104, Alan R Liss, New York
27 Navon, G , Shulman, R G , Yamane, T., Eccleshall, T.R , Lam, K -B., Baronofsky, J.J and Marmur, J (1979) Biochemistry 18, 4487–4499
28 Den Hollander, J A , Ugurbil, K , Brown, T R and Shulman, R.G (1981) Biochemistry 20, 5871–5880
29 Gillies, R J , Ugurbil, K , Den Hollander, J.A and Shulman, R G (1981) Proc Natl Acad Sci USA 78, 2125–2129

30 Ogino, T., Den Hollander, J.A. and Shulman, R.G. (1983) Proc. Natl. Acad. Sci. USA 80, 5185–5189
31 Nicolay, K., Scheffers, W.A., Bruinenberg, P.M. and Kaptein, R. (1982) Arch. Microbiol. 133, 83–89
32 Nicolay, K., Scheffers, W.A., Bruinenberg, P.M. and Kaptein, R. (1983) Arch. Microbiol. 134, 270–275
33 Alger, J.R., Den Hollander, J.A. and Shulman, R.G. (1982) Biochemistry 21, 2957–2963
34 Eddy, A.A., Indge, K.J., Backen, K. and Nowacki, J.A. (1970) Biochem. J. 120, 845–852
35 Hansen, U.-P., Gradmann, G., Sanders, D. and Slayman, C.L. (1981) J. Membrane Biol. 63, 165–190
36 Slayman, C.L. and Slayman, C.W. (1968) J. Gen. Physiol. 52, 424–443
37 Seaston, A., Inkson, C. and Eddy, A.A. (1973) Biochem. J. 134, 1031–1043
38 Cockburn, M., Earnshaw, P. and Eddy, A.A. (1975) Biochem. J. 146, 705–712
39 Kotyk, A. and Rihova, L. (1972) Biochim. Biophys. Acta 288, 380–389
40 Marquardt, D.W. (1963) J. Soc. Ind. Appl. Math. 11, 431–441
41 Hansen, U.-P., Gradmann, D., Tittor, J., Sanders, D. and Slayman, C.L. (1982) in Plasmalemma and Tonoplast: Their Functions in the Plant Cell (Marmé, D., Marrè, E. and Hertel, R., eds.), pp. 77–84, Elsevier Biomedical Press, Amsterdam
42 Läuger, P. and Stark, G. (1970) Biochim. Biophys. Acta 211, 458–466
43 Borst-Pauwels, G.W.F.H. (1981) Biochim. Biophys. Acta 650, 88–127
44 Slayman, C.L. (1973) J. Bacteriol. 114, 752–766
45 Slayman, C.L., Long, W.S. and Lu, C.Y.-H. (1973) J. Membrane Biol. 14, 305–338
46 Slayman, C.L. (1980) in Plant Membrane Transport: Current Conceptual Issues (Spanswick, R.M., Lucas, W.J. and Dainty, J., eds.), pp. 179–190, Elsevier, Amsterdam
47 Eddy, A.A., Philo, R., Earnshaw, P. and Brocklehurst, R. (1977) in Biochemistry of Membrane Transport, FEBS Symposium No. 42 (Semenza, G. and Carafoli, E., eds.), pp. 250–260, Springer-Verlag, Berlin
48 Sanders, D., Slayman, C.L. and Pall, M.L. (1983) Biochim. Biophys. Acta 735, 67–76
49 Kimmich, G.A. and Randles, J. (1980) Biochim. Biophys. Acta 596, 439–444
50 Wiemken, A. and Dürr, M. (1974) Arch. Microbiol. 101, 45–57
51 Urech, K., Dürr, M., Boller, T. and Wiemken, A. (1978) Arch. Microbiol. 116, 275–278
52 Okorokov, L.A., Lichko, L.P. and Kulaev, I.S. (1980) J. Bacteriol. 144, 661–665
53 Sigler, K., Knotková, A. and Kotyk, A. (1981) Biochim. Biophys. Acta 643, 572–582